ACS Photonics

pubs.acs.org/journal/apchd5

Letter

# Transverse Electric Lasing at a Record Short Wavelength 244.63 nm from GaN Quantum Wells with Weak Exciton Localization

Maocheng Shan, Yi Zhang, Ming Tian, Rongyu Lin, Jie'an Jiang, Zhihua Zheng, Yongming Zhao, Yi Lu, Zhechuan Feng, Wei Guo, Jiangnan Dai, Changqing Chen,* Feng Wu,* and Xiaohang Li*

Cite This: *ACS Photonics* 2021, 8, 1264−1270

Read Online

ACCESS | Metrics & More | Article Recommendations | Supporting Information

**ABSTRACT:** We have demonstrated a record short wavelength lasing at 244.63 nm with TE dominant polarization from GaN quantum wells (QWs) at room temperature (RT). The optical threshold of 310 kW/cm$^2$ is comparable to state-of-the-art AlGaN QW lasers at similar wavelengths. The sample was grown on the AlN/sapphire template pesudomorphically. X-ray diffraction (XRD) shows unambiguous higher-order satellite peaks indicating a sharp interface amid the active region. The excitonic localization was revealed and studied by the photoluminescence (PL) and time-resolved PL (TRPL) spectroscopy at temperatures ranging from 15 K to RT. At 15 K, the multiple-component PL decay curves with the decay time varying from 62.6 to 2.77 ns at different energies confirmed the localized excitons. The peak energy of the temperature-dependent PL spectra exhibited the "S-shape" behavior; and the weak exciton localization with a small localization energy of 14.3 meV was observed. Therefore, even in the low temperature region, the escape possibility of excitons increased as the temperature rose. As a result, the fwhm of the emission spectra changed significantly when the temperature was below 150 K. Above 150 K, the PL decay shape changed from the two-component exponential decay to the single exponential decay, indicating complete delocalization of excitons. The work demonstrates the weak localization and thus smooth interface in the GaN/AlN active region, which are desirable for DUV lasers operating at RT.

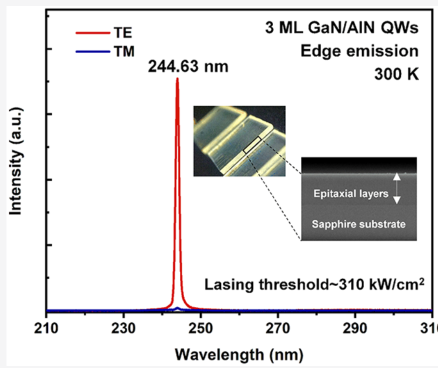


**KEYWORDS:** *DUV lasers, GaN/AlN quantum wells, transverse electric polarization, exciton localization, time-resolved photoluminescence, MOCVD*

Deep ultraviolet (DUV) lasers based on the AlGaN quantum well (QWs) have been extensively investigated for their critical applications in covert communication, spectral analysis, optical storage, medical diagnostics, and so on.[1−3] The current injected AlGaN QW DUV laser at 271.8 nm has been developed on the bulk AlN substrate.[4] In addition, the optically pumped AlGaN QW lasers have reached down to 237 nm.[5−7] However, due to the valence sub-bands crossover of AlGaN,[8] the optical polarization of DUV lasers switches from the transverse electric (TE) mode to the transverse magnetic (TM) mode when the emission wavelengths were shorter than 238 and 249 nm on less available AlN and more available sapphire substrates, respectively.[9,10] The switch of the optical polarization to TM could compromise the laser performance as the TM mode suffers from lower facet reflectivity and could be more easily absorbed by the p-type layers and metals due to wider optical modes.[8,9] Another caveat of the AlGaN QWs is the quantum confined Stark effect (QCSE) that occurs in the several nm thick AlGaN QW. It could reduce the overlap of electron and hole wave functions and thus the optical gain.

Recently, the ultrathin GaN/AlN binary QWs have emerged as a promising candidate for UV lasers and light-emitting diodes (LEDs) that can address the issues of the AlGaN QWs above.[11−13] Via tuning the well width from one to a few monolayers (MLs), the effective transition energy of GaN/AlN QWs could be adjusted due to the extremely large band offset and thus strong quantum confinement.[14−17] Using such GaN QWs, the LEDs with wavelengths ranging from 365 to 219 nm have been demonstrated.[17−22] Importantly, the optical polarization switch from TE to TM at shorter wavelengths could be eliminated thanks to the nature of the valence band of GaN, where the split-off hole band situates below the heavy and light hole bands to ensure TE dominant polarization.[21] Furthermore, the QCSE is reduced as a result of the extreme quantum confinement in the ultrathin and deep GaN QWs.[22]

However, whether grown by metal organic chemical vapor deposition (MOCVD) or molecular beam epitaxy (MBE), the controlled epitaxy of high quality GaN ML in the AlN matrix has still remained elusive.[20,23] For instance, the thickness

**Received:** January 17, 2021
**Published:** April 16, 2021

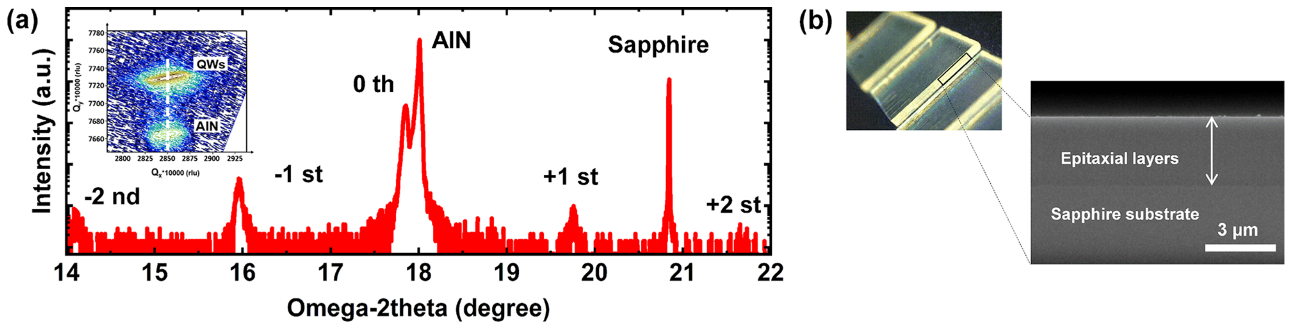


**Figure 1.** (a) XRD $\omega$-2$\theta$ scan with the inset showing asymmetric (105) RSM of the GaN/AlN laser structure. (b) Photograph of cleaved laser bars and SEM image of the cleaved facet.

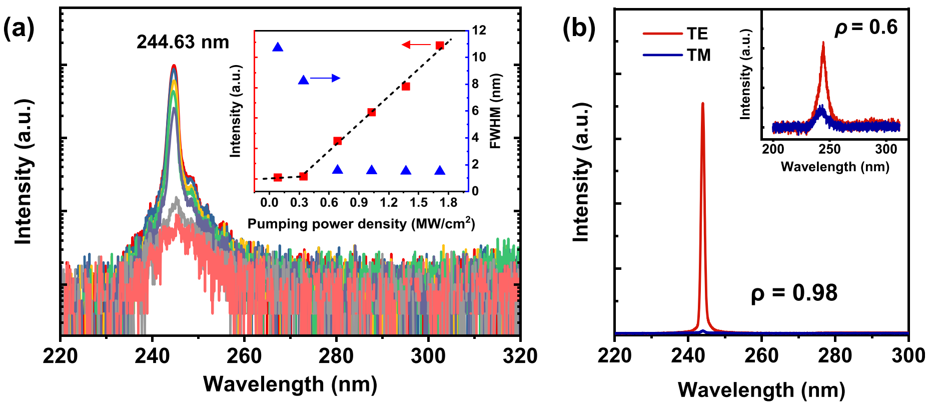


**Figure 2.** (a) Laser emission spectra with the inset being peak intensity and line width of the spectra as a function of pumping power density. (b) The stimulated emission and spontaneous emission (inset) of the laser both show TE-dominant polarization.

fluctuations and size distribution have been widely observed in the GaN/AlN QWs. These inhomogeneities create a fluctuated potential profile due to modulation of the quantum confinement energy, which results in the in-plane exciton localization and thus the red-shift, inhomogeneous broadening, and multiple peaks emission spectrum.[24,25] In addition, for lasers, the large localization energy could increase the threshold and reduce the slope efficiency.[26,27] Therefore, the weak localization and thus smooth well−barrier interface are crucial for the DUV lasers based on the GaN/AlN QWs. Currently, the range of 2−4 ML thickness fluctuations of the GaN/AlN QWs has been confirmed by the morphological characterization, that is, the cross-sectional transmission electron microscopy (TEM) or high-angle annular dark-field scanning TEM (HAADF-STEM).[20] However, there is a lack of optical characterization of the localized excitons in the GaN/AlN QWs, let alone the localization depth and its impact on lasers. In addition to the reports on the GaN QW UV LEDs, the first DUV laser based on the GaN QWs have been demonstrated at 249 nm.[28] This wavelength is equal to the shortest wavelength of the AlGaN QW laser with the TE polarization on the sapphire substrate.[6]

In this work, we have demonstrated lasing at 244.63 nm with TE polarization from the 3 ML GaN/AlN QWs grown by MOCVD on the sapphire substrate, a record short wavelength from the GaN/AlN QWs to date. We further investigated the spectral characteristics of localized excitons in the GaN/AlN QWs by the energy-dependent time-resolved photoluminescence (TRPL), temperature-dependent steady-state PL and TRPL measurements. Through the investigations of carrier dynamics, the depth of the localization was obtained and its impact on the laser was analyzed.

The active region of the laser comprising 40 periods of the GaN/AlN QWs was sandwiched by a 3 $\mu$m AlN template and a 10 nm AlN cap, which was grown on a *c*-plane sapphire substrate by MOCVD. The source precursors for the growth were trimethylaluminum, trimethylgallium, and ammonia, with hydrogen as the carrier gas. To probe the interface roughness and estimate the thickness of the GaN/AlN QWs, the symmetric XRD $\omega$-2$\theta$ scan was performed and illustrated in Figure 1a. The steep higher-order satellite peaks demonstrate the pronounced periodical structures with sharp interfaces. The thickness of the GaN wells and the AlN barriers was estimated to be 3 and 5.5 MLs, respectively, according to the growth rate and the previous work.[28] The thicknesses of the wells and barriers were designed from the trade-off between the wavelength, quantum confinement, optical confinement, and light absorption of the optical pumping source by a 193 nm ArF excimer laser. The optical confinement of the 40 period GaN/AlN (3 MLs/5.5 MLs) QW laser was estimated to be 27.2% through calculation of the optical field distribution by the COMSOL Multiphase software package. The detailed descriptions of the sample design, growth, simulation and preparation could be found in the Supporting Information. Moreover, the XRD asymmetric (105) reciprocal space mapping (RSM) shown in the inset of Figure 1a manifests the pseudomorphic growth of the GaN/AlN QWs on the AlN/sapphire template, indicating that the active region is compressively strained on the AlN/sapphire template, beneficial for maintaining the lower position of the split-off hole band for TE dominant polarization.[28]


https://doi.org/10.1021/acsphotonics.1c00090
ACS Photonics 2021, 8, 1264−1270

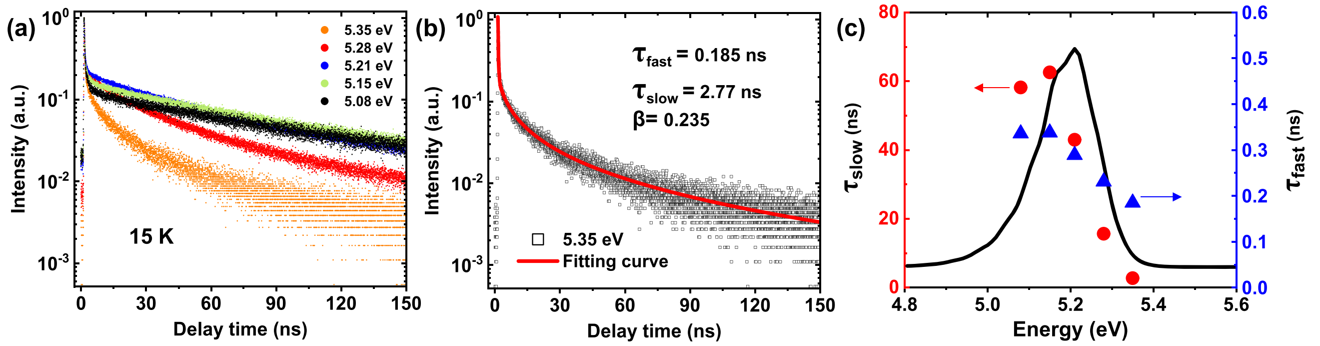


**Figure 3.** (a) PL decay curves at different photon energies measured at 15 K. (b) Typical fitting of the decay curve at 5.35 eV by eq 1. (c) Fast and slow PL decay times as a function of the monitored photon energy.

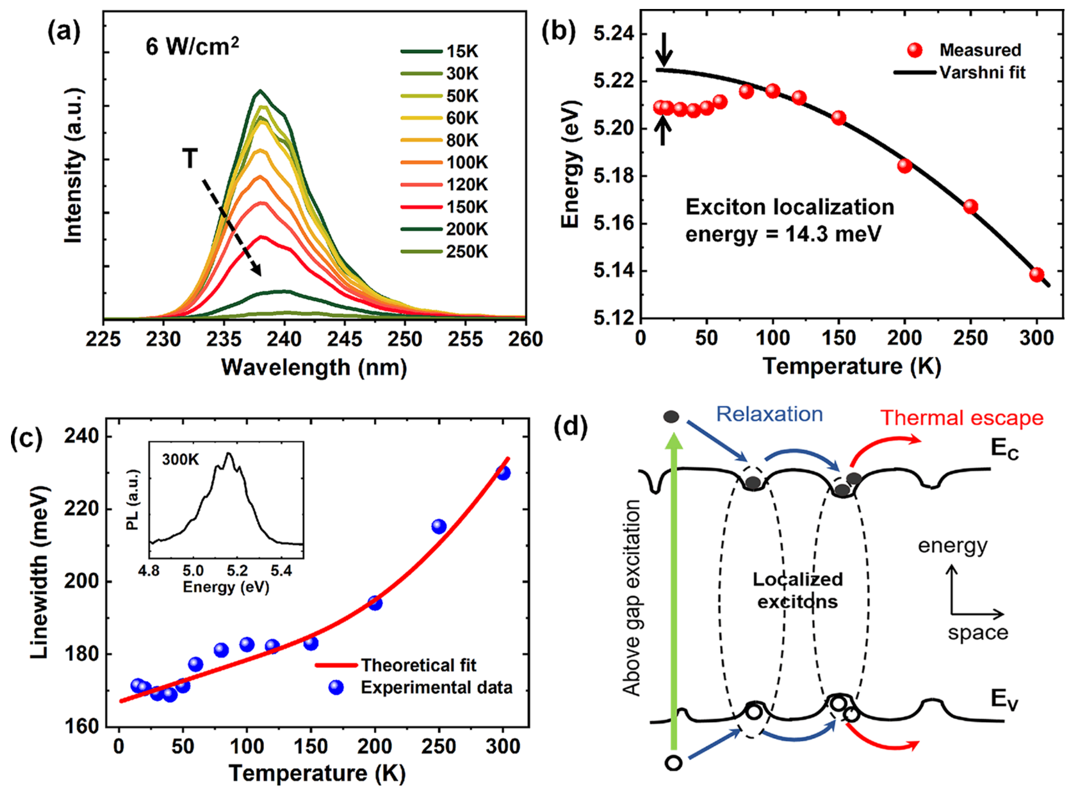


**Figure 4.** (a) Temperature-dependent PL spectra from 15 to 250 K. Variation of (b) emission energy and (c) line width of the PL spectra with temperature, with the PL spectrum at 300 K shown in the inset. (d) Schematic drawing of the weakly localized excitons in GaN/AlN QWs.

Next, the epitaxial wafer was prepared into individual laser bars shown in Figure 1b with the cavity length of 1 mm for optical pumping. The edge-emitting cavities were cleaved along the *m*-plane of the epitaxial layers with the assistance of laser scribing on the backside of sapphire substrate. The smooth Fabry-Pérot facets were manifested by the cross-sectional scanning electronic microscopy (SEM) shown in Figure 1b. No additional mirrors were applied. Subsequently, the optically pumped experiments were performed using an 193 nm ArF excimer laser (5 ns pulses at 50 Hz). The edge emissions were detected near one facet by a charge-coupled device (CCD) camera through a Horiba iHR550 spectrometer. As the pumping power density increased from 80 to 1700 kW/cm$^2$, a narrowed DUV lasing at 244.63 nm was observed, as illustrated in Figure 2a. The peak intensity and line width of the spectra illustrate the distinct threshold of 310 kW/cm$^2$, which is comparable to the state-of-the-art AlGaN QW lasers at similar wavelengths.[9] The degrees of polarization ($\rho$), defined as $\rho = (I_{TE} - I_{TM})/(I_{TE} + I_{TM})$, are 0.98 and 0.6 for the stimulated emission and spontaneous emission, respectively, shown in Figure 2b, which demonstrated the TE-dominant polarization of the 244.63 nm GaN/AlN QW laser. This TE-dominant lasing wavelength is the shortest among the reported DUV lasers grown on sapphire substrates, including the AlGaN QW lasers.[6]

To investigate the interface fluctuations and thus the localized excitons of the GaN/AlN QW, the steady-state PL and TRPL measurements were performed with varying temperature using a He-closed cycle cryostat. A diode pumped all-solid-state picosecond pulsed laser operating at 213 nm was applied as the excitation source, with repetition frequency of 5 MHz and pulse width <50 ps. The average excitation power density was 6 W/cm$^2$. The TRPL signals were recorded perpendicular to the *c*-plane surface by a time-correlated



https://doi.org/10.1021/acsphotonics.1c00090
ACS Photonics 2021, 8, 1264−1270

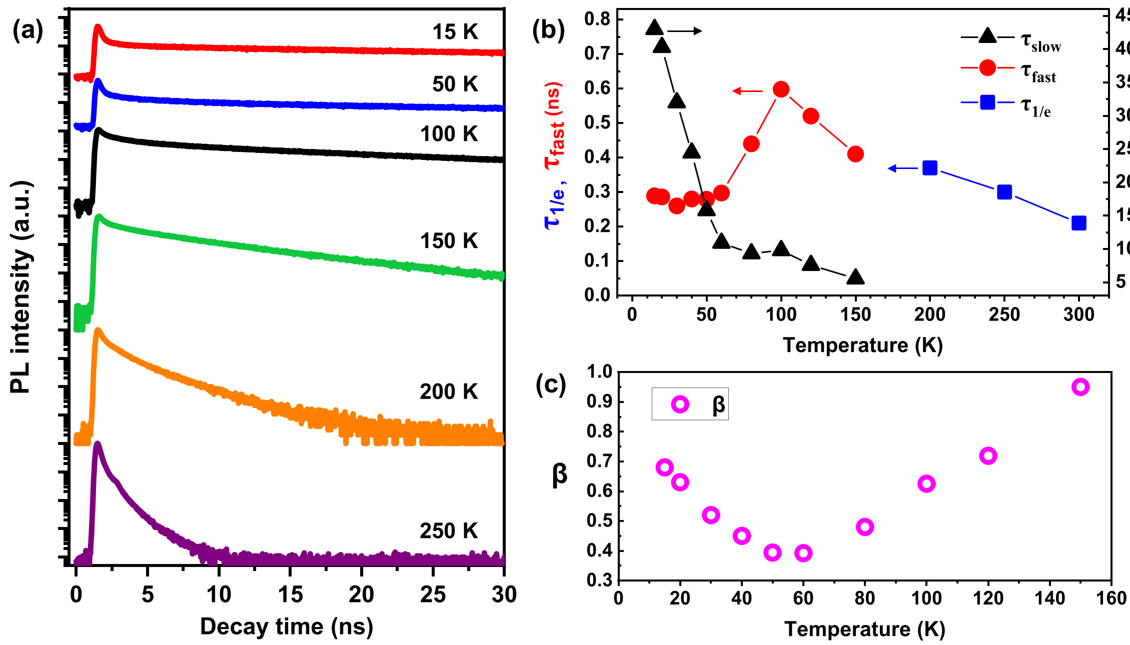


**Figure 5.** (a) TD-TRPL decay curves at representative temperatures at 5.21 eV. Variation of (b) the fitted decay times and (c) $\beta$ with temperature.

single-photon counting system. Figure 3a shows the PL decay curves at different photon energy at 15 K. These curves clearly consist of two decay components: a fast initial decay and a prolonged slow decay. The highly nonexponential decay varies across the PL spectrum, and the variation of decay time has been interpreted by the fluctuations of the localization energy.[11] However, these transients do not match either the biexponential or stretched exponential decay models, which have been widely utilized to analyze the exciton localization.[29,30] To get insight into the decay curves, the experiment data was well fitted, shown in Figure 3b, by a combined exponential and stretched exponential line shape:[31−33]

$$I(t) = A_{\text{fast}} \exp\left(-\frac{t}{\tau_{\text{fast}}}\right) + A_{\text{slow}} \exp\left[\left(-\frac{t}{\tau_{\text{slow}}}\right)^{\beta}\right] \tag{1}$$

$I(t)$ is the time-dependent PL intensity. $\tau_{\text{fast}}$ and $\tau_{\text{slow}}$ are the fast and slow decay times, respectively. $A_{\text{fast}}$ and $A_{\text{slow}}$ are the weights of the corresponding decay term. $\beta$ is the dimensionality of the localization. This model has been applied to analyze the decay shape of the localized excitons in InGaN/GaN QWs grown on the nonpolar substrate.[31,32] Since the initial decay dominates the overall PL, the fast decay time was considered to express the recombination lifetime of excitons from free or extended states to the localized centers; and the slow decay time accounts for the relaxation of excitons among localized states.[34] Despite that the QCSE is greatly reduced in QWs on nonpolar substrate due to the lack of polarization, the initial stage of the GaN/AlN QWs decays faster than that of the nonpolar InGaN/GaN QWs.[34] This behavior is mostly attributed to the strong quantum confinement in the ultrathin QWs and, thus, the increased oscillator strength. The fitted decay times at different energies are illustrated in Figure 3c. One can see that $\tau_{\text{slow}}$ decreases rapidly with increasing emission energy, indicating that the decay of localized excitons is due to not only radiative recombination, but also the relaxation process of the tail state.[35] For lower energy, deep localization states more effectively suppress the in-plane relaxation of excitons, which accounts for the long-lived tail with a decay time of tens of ns at low temperature. In contrast, $\tau_{\text{fast}}$ varies little, shortened by only tens of ps as the energy increases, which is attributed to the reduced QCSE of weak localization states of thin QWs. The dependence of the lifetime on the photon energy verifies the localized excitons in the GaN/AlN QWs.

Figure 4a plots the temperature-dependent (TD) PL spectra measured at the average excitation power density of 6 W/cm$^2$. The abnormal feature in the data is the increased PL intensity at 50 K versus the one at 30 K, probably caused by the redistribution of excitons in the local environment,[16] and the details are discussed later. A rapid quenching of the PL intensity is shown at temperatures above 150 K, which indicates the increased amount of nonradiative recombination due to the defect trapping of excitons. The shift of PL peak wavelength with temperature is illustrated in Figure 4b, which presents an S-shaped dependence. To analyze the depth of the localization, the experiment data was fitted by the Varshni empirical formula: $E_g(T) = E_g(0) - \alpha T^2/(\beta + T)$,[19] where $E_g(0)$ is the bandgap energy of GaN/AlN QWs at 0 K and $\alpha$ and $\beta$ are the fitting parameters. From the difference between fitting and experimental peak energy at lowest temperature, the exciton localization energy ($E_{\text{loc}}$) of 14.3 meV was obtained, as indicated by the double arrows in Figure 4b. The 14.3 meV $E_{\text{loc}}$ is smaller than the thermal energy of ~25 meV at RT. Thus, the weakly localized excitons can escape when they get a certain amount of thermal energy to overcome the distributed potential barriers.

Therefore, the fwhm of the PL spectra exhibits a fluctuating behavior when the temperature varies from low to high, shown in Figure 4c. The solid line shows that the fwhm increases monotonically with temperature, without the effect of localization, as expressed by the following relation:[27,36]

$$\Gamma(T) = \Gamma(0) + aT + b/\left[\exp\left(\frac{\hbar\omega_{\text{LO}}}{k_B T}\right) - 1\right] \tag{2}$$



https://doi.org/10.1021/acsphotonics.1c00090
ACS Photonics 2021, 8, 1264−1270

$\Gamma(0)$ is the temperature-independent contribution to the line width, and $aT$ is the contribution of acoustic phonon. The last term is due to the scattering with longitudinal optical (LO) phonon. For simplicity, $\hbar\omega_{LO}$ is fixed as the LO phonon energy of GaN.[37] Below 150 K, the discrepancy between the theoretical fitting curve and the experimental data is due to the effect of exciton localization. As temperature increases from 15 K, photogenerated excitons relax to the distributed potential minima, as indicated by the blue arrows in Figure 4d, resulting in a decreasing trend of the fwhm with the smallest value of 168 meV at 40 K. With a further increase of temperature (50 K < $T$ < 100 K), localized excitons are partially thermalized to occupy the higher energy states, which leads to the blue shift of the PL peak energy in Figure 4b as well as the increase of the fwhm in Figure 4c. The equilibrium energy distribution is gradually approached in the temperature range of 100−150 K, and the fwhm basically remains constant. However, at sufficiently high temperature, that is, beyond 150 K, excitons are thermally activated and delocalize from the potential minima as shown by the red arrows in Figure 4d, and the fwhm increases in accordance with the thermal broadening of the PL spectra. The inset of Figure 4c shows the multiple peaks PL spectrum with the largest fwhm of 230 meV at RT, which reveals the absence of the effective localization. The discussion above suggests the relatively weak localization caused by the interface fluctuations in the active region of the laser.

To further confirm the influence of the thermal effect on exciton relaxation and delocalization process, TD-TRPL measurements were carried. Figure 5a shows the evolution of the PL decay curves at 5.21 eV. Utilizing eq 1, the fitted $\tau_{fast}$ and $\tau_{slow}$ are plotted in Figure 5b. It should be noted that the model of the combined exponential and stretched exponential decay shape can fit the curves at and below 150 K. Above 150 K, the slow decay component disappears, and the model is not applicable. In Figure 5a, the fast decay shape remains unchanged at temperatures below 50 K, as the emission originates from radiative recombination of excitons confined in the potential minima. With temperatures over 50 K, the fast decay slows down because of the occupation of excitons from lower-lying states to higher energy states near the PL peak energy. The redistributed excitons increase the PL intensity, thus, slowing down the decay rate, leading to the increasing $\tau_{fast}$ above 50 K. Such a temporal behavior caused by the exciton transport between different energy states was also observed in the InGaN/GaN QWs and other disorder alloys.[38,39] However, when excitons are thermally activated to escape from the localization sites, $\tau_{fast}$ is thereby reduced above 100 K. Above 150 K, the excitons are fully delocalized and the decay shape changes to a single exponential decay with an effective lifetime defined as $\tau_{1/e}$. Figure 5c shows the value of $\beta$ as a function of the temperature. Generally, the value of $\beta$ corresponds to the lifetime distribution describing the fundamental relaxation process, whether they are radiative or nonradiative.[40] At low temperature, $\beta$ decreases first due to exciton relaxation to the localized states. As the temperature goes up, the escape process is thermally activated and $\beta$ increases. These discussions agree well with the results of TD-PL in Figure 4a−c. Therefore, in terms of the threshold and slope efficiency (Figure 2a), the 3 ML GaN/AlN QWs with weak exciton localization are consequently desirable for DUV lasers operating at RT.

In conclusion, we have demonstrated lasing at a record-short wavelength of 244.63 nm with TE polarization from the 3 ML GaN/AlN QWs on sapphire substrate. A low threshold of 310 kW/cm$^2$ was obtained, which is comparable to state-of-the-art AlGaN QW lasers at similar wavelengths. The XRD analysis shows the coherence and sharp interfaces of the GaN/AlN QWs. The weak exciton localization caused by the fluctuated potential profile was revealed and investigated by the PL and TRPL spectroscopy from 15 K to RT. At 15 K, the PL decay curves comprised multiple components; and the decay time varied from 62.6 to 2.77 ns at different energies, indicating the localized excitons. The "S-shape" behavior of the peak energy shift of the TD-PL spectra was attributed to the weak exciton localization with $E_{loc}$ of 14.3 meV. Therefore, due to thermal activation, the excitons occupied higher energy states and finally escaped from the localized states as the temperature increased. As a result, the fwhm of the emission spectra exhibited a decreasing−increasing behavior when the temperature was below 150 K. Above 150 K, the PL decay shape changed from the two-component exponential decay to the single exponential decay, which confirmed the complete delocalization of excitons. This work demonstrates the weak exciton localization and thus smooth interface in the GaN/AlN active region which are suitable to yield high performance DUV lasers at RT.

## ■ ASSOCIATED CONTENT

### Supporting Information

The Supporting Information is available free of charge at https://pubs.acs.org/doi/10.1021/acsphotonics.1c00090.

(I) Details of the sample growth; (II) Descriptions of the sample design; (III) Simulations of the optical confinement; (IV) Preparation of the laser bars (PDF)

## ■ AUTHOR INFORMATION


### Corresponding Authors

**Changqing Chen** − *Wuhan National Laboratory for Optoelectronics, Huazhong University of Science and Technology, Wuhan 430074, People's Republic of China*; Email: cqchen@hust.edu.cn

**Feng Wu** − *Wuhan National Laboratory for Optoelectronics, Huazhong University of Science and Technology, Wuhan 430074, People's Republic of China*; Email: wu_wufeng@126.com

**Xiaohang Li** − *King Abdullah University of Science and Technology (KAUST), Advanced Semiconductor Laboratory, Thuwal 23955, Saudi Arabia*; orcid.org/0000-0002-4434-365X; Email: xiaohang.li@kaust.edu.sa

### Authors

**Maocheng Shan** − *Wuhan National Laboratory for Optoelectronics, Huazhong University of Science and Technology, Wuhan 430074, People's Republic of China; King Abdullah University of Science and Technology (KAUST), Advanced Semiconductor Laboratory, Thuwal 23955, Saudi Arabia*

**Yi Zhang** − *Wuhan National Laboratory for Optoelectronics, Huazhong University of Science and Technology, Wuhan 430074, People's Republic of China*

**Ming Tian** − *College of Physics Science and Technology, Guangxi Key Laboratory for the Relativistic Astrophysics,*



https://doi.org/10.1021/acsphotonics.1c00090
ACS Photonics 2021, 8, 1264−1270

Laboratory of Optoelectronic Materials and Detection Technology, Guangxi University, Nanning 530004, China

**Rongyu Lin** − *King Abdullah University of Science and Technology (KAUST), Advanced Semiconductor Laboratory, Thuwal 23955, Saudi Arabia*

**Jie'an Jiang** − *Ningbo Institute of Materials Technology and Engineering, Chinese Academy of Sciences, Ningbo 315201, Zhejiang, China*

**Zhihua Zheng** − *Wuhan National Laboratory for Optoelectronics, Huazhong University of Science and Technology, Wuhan 430074, People's Republic of China*

**Yongming Zhao** − *Wuhan National Laboratory for Optoelectronics, Huazhong University of Science and Technology, Wuhan 430074, People's Republic of China*

**Yi Lu** − *King Abdullah University of Science and Technology (KAUST), Advanced Semiconductor Laboratory, Thuwal 23955, Saudi Arabia*

**Zhechuan Feng** − *College of Physics Science and Technology, Guangxi Key Laboratory for the Relativistic Astrophysics, Laboratory of Optoelectronic Materials and Detection Technology, Guangxi University, Nanning 530004, China*

**Wei Guo** − *Ningbo Institute of Materials Technology and Engineering, Chinese Academy of Sciences, Ningbo 315201, Zhejiang, China;* orcid.org/0000-0002-6233-0529

**Jiangnan Dai** − *Wuhan National Laboratory for Optoelectronics, Huazhong University of Science and Technology, Wuhan 430074, People's Republic of China;* orcid.org/0000-0001-9805-8726

Complete contact information is available at: https://pubs.acs.org/10.1021/acsphotonics.1c00090

### Notes

The authors declare no competing financial interest.

## ■ ACKNOWLEDGMENTS

This work is supported by the National Key Research and Development Program of China (Grant No. 2016YFB0400901), the Center of Micro-Fabrication and Characterization (CMFC) of WNLO, Chinese Academy of Sciences (Grant No. IIMDKFJJ-17-09), the National Natural Science Foundation of China (Grant Nos. 61704062, 61774065, and 61704176), the China Postdoctoral Science Foundation (Grant No. 2016M602287), and the Director Fund of WNLO. The KAUST authors appreciate the support of KAUST Baseline BAS/1/1664-01-01, GCC Research Council REP/1/3189-01-01, and Competitive Research Grants URF/1/3437-01-01 and URF/1/3771-01-01.

## ■ REFERENCES

(1) Yoshida, H.; Yamashita, Y.; Kuwabara, M.; Kan, H. Demonstration of an Ultraviolet 336 nm AlGaN Multiple-Quantum-Well Laser Diode. *Appl. Phys. Lett.* **2008**, *93* (24), 241106.

(2) Martens, M.; Kuhn, C.; Simoneit, T.; Hagedorn, S.; Knauer, A.; Wernicke, T.; Weyers, M.; Kneissl, M. The Effects of Magnesium Doping on the Modal Loss in AlGaN-Based Deep UV Lasers. *Appl. Phys. Lett.* **2017**, *110* (8), 081103.

(3) Li, X.; Xie, H.; Ponce, F. A.; Ryou, J.-H.; Detchprohm, T.; Dupuis, R. D. Onset of Surface Stimulated Emission at 260 nm from AlGaN Multiple Quantum Wells. *Appl. Phys. Lett.* **2015**, *107* (24), 241109.

(4) Zhang, Z.; Kushimoto, M.; Sakai, T.; Sugiyama, N.; Schowalter, L. J.; Sasaoka, C.; Amano, H. A 271.8 nm Deep-Ultraviolet Laser Diode for Room Temperature Operation. *Appl. Phys. Express* **2019**, *12* (12), 124003.

(5) Kao, T.-T.; Liu, Y.-S.; Mahbub Satter, Md; Li, X.-H.; Lochner, Z.; Douglas Yoder, P.; Detchprohm, T.; Dupuis, R. D.; Shen, S.-C.; Ryou, J.-H.; Fischer, A. M.; Wei, Y.; Xie, H.; Ponce, F. A. Sub-250 nm Low-Threshold Deep-Ultraviolet AlGaN-Based Heterostructure Laser Employing $HfO_2/SiO_2$ Dielectric Mirrors. *Appl. Phys. Lett.* **2013**, *103* (21), 211103.

(6) Li, X.-H.; Detchprohm, T.; Kao, T.-T.; Satter, Md. M.; Shen, S.-C.; Douglas Yoder, P.; Dupuis, R. D.; Wang, S.; Wei, Y. O.; Xie, H.; Fischer, A. M.; Ponce, F. A.; Wernicke, T.; Reich, C.; Martens, M.; Kneissl, M. Low-Threshold Stimulated Emission at 249 and 256 nm from AlGaN-Based Multiple-Quantum-Well Lasers Grown on Sapphire Substrates. *Appl. Phys. Lett.* **2014**, *105* (14), 141106.

(7) Martens, M.; Mehnke, F.; Kuhn, C.; Reich, C.; Kueller, V.; Knauer, A.; Netzel, C.; Hartmann, C.; Wollweber, J.; Rass, J.; Wernicke, T.; Bickermann, M.; Weyers, M.; Kneissl, M. Performance Characteristics of UV-C AlGaN-Based Lasers Grown on Sapphire and Bulk AlN Substrates. *IEEE Photonics Technol. Lett.* **2014**, *26* (4), 342−345.

(8) Kawanishi, H.; Senuma, M.; Nukui, T. Anisotropic Polarization Characteristics of Lasing and Spontaneous Surface and Edge Emissions from Deep-Ultraviolet ($\lambda \approx 240$ nm) AlGaN Multiple-Quantum-Well Lasers. *Appl. Phys. Lett.* **2006**, *89* (4), 041126.

(9) Li, X.-H.; Kao, T.-T.; Satter, Md. M.; Wei, Y. O.; Wang, S.; Xie, H.; Shen, S.-C.; Yoder, P. D.; Fischer, A. M.; Ponce, F. A.; Detchprohm, T.; Dupuis, R. D. Demonstration of Transverse-Magnetic Deep-Ultraviolet Stimulated Emission from AlGaN Multiple-Quantum-Well Lasers Grown on a Sapphire Substrate. *Appl. Phys. Lett.* **2015**, *106* (4), 041115.

(10) Lachab, M.; Sun, W.; Jain, R.; Dobrinsky, A.; Gaevski, M.; Rumyantsev, S.; Shur, M.; Shatalov, M. Optical Polarization Control of Photo-Pumped Stimulated Emissions at 238 nm from AlGaN Multiple-Quantum-Well Laser Structures on AlN Substrates. *Appl. Phys. Express* **2017**, *10* (1), 012702.

(11) Furis, M.; Cartwright, A. N.; Wu, H.; Schaff, W. J. Room-Temperature Ultraviolet Emission from GaN/AlN Multiple-Quantum-Well Heterostructures. *Appl. Phys. Lett.* **2003**, *83* (17), 3486−3488.

(12) Bayerl, D.; Kioupakis, E. Room-Temperature Stability of Excitons and Transverse-Electric Polarized Deep-Ultraviolet Luminescence in Atomically Thin GaN Quantum Wells. *Appl. Phys. Lett.* **2019**, *115* (13), 131101.

(13) Toropov, A. A.; Evropeitsev, E. A.; Nestoklon, M. O.; Smirnov, D. S.; Shubina, T. V.; Kaibyshev, V. Kh; Budkin, G. V.; Jmerik, V. N.; Nechaev, D. V.; Rouvimov, S.; Ivanov, S. V.; Gil, B. Strongly Confined Excitons in GaN/AlN Nanostructures with Atomically Thin GaN Layers for Efficient Light Emission in Deep-Ultraviolet. *Nano Lett.* **2020**, *20* (1), 158−165.

(14) Growden, T. A.; Storm, D. F.; Cornuelle, E. M.; Brown, E. R.; Zhang, W.; Downey, B. P.; Roussos, J. A.; Cronk, N.; Ruppalt, L. B.; Champlain, J. G.; Berger, P. R.; Meyer, D. J. Superior Growth, Yield, Repeatability, and Switching Performance in GaN-Based Resonant Tunneling Diodes. *Appl. Phys. Lett.* **2020**, *116* (11), 113501.

(15) Wang, Y.; Rong, X.; Ivanov, S.; Jmerik, V.; Chen, Z.; Wang, H.; Wang, T.; Wang, P.; Jin, P.; Chen, Y.; Kozlovsky, V.; Sviridov, D.; Zverev, M.; Zhdanova, E.; Gamov, N.; Studenov, V.; Miyake, H.; Li, H.; Guo, S.; Yang, X.; Xu, F.; Yu, T.; Qin, Z.; Ge, W.; Shen, B.; Wang, X. Deep Ultraviolet Light Source from Ultrathin GaN/AlN MQW Structures with Output Power Over 2 W. *Adv. Opt. Mater.* **2019**, *7* (10), 1801763.

(16) Aiello, A.; Wu, Y.; Pandey, A.; Wang, P.; Lee, W.; Bayerl, D.; Sanders, N.; Deng, Z.; Gim, J.; Sun, K.; Hovden, R.; Kioupakis, E.; Mi, Z.; Bhattacharya, P. Deep Ultraviolet Luminescence Due to Extreme Confinement in Monolayer GaN/Al(Ga)N Nanowire and Planar Heterostructures. *Nano Lett.* **2019**, *19* (11), 7852−7858.

(17) Islam, S. M.; Lee, K.; Verma, J.; Protasenko, V.; Rouvimov, S.; Bharadwaj, S.; Xing, H.; Jena, D. MBE-Grown 232−270 nm Deep-UV LEDs Using Monolayer Thin Binary GaN/AlN Quantum Heterostructures. *Appl. Phys. Lett.* **2017**, *110* (4), 041108.

(18) Subedi, R. C.; Min, J.-W.; Mitra, S.; Li, K.-H.; Ajia, I.; Stegenburgs, E.; Anjum, D. H.; Conroy, M.; Moore, K.; Bangert, U.; Roqan, I. S.; Ng, T. K.; Ooi, B. S. Quantifying the Transverse-Electric-Dominant 260 nm Emission from Molecular Beam Epitaxy-Grown GaN-Quantum-Disks Embedded in AlN Nanowires: A Comprehensive Optical and Morphological Characterization. *ACS Appl. Mater. Interfaces* **2020**, *12* (37), 41649−41658.

(19) Wu, F.; Zhang, J.; Wang, S.; Long, H.; Dai, J.; Feng, Z. C.; Gong, Z.; Chen, C. Quantum Confinement Dependence of Exciton Localization in A-Plane GaN/AlGaN Multiquantum Wells Investigated by Temperature Dependent Photoluminescence. *Opt. Mater. Express* **2015**, *5* (11), 2608.

(20) Liu, C.; Ooi, Y. K.; Islam, S. M.; Verma, J.; Xing, H.; Jena, D.; Zhang, J. Physics and Polarization Characteristics of 298 nm AlN-Delta-GaN Quantum Well Ultraviolet Light-Emitting Diodes. *Appl. Phys. Lett.* **2017**, *110* (7), 071103.

(21) Liu, C.; Ooi, Y. K.; Islam, S. M.; Xing, H.; Jena, D.; Zhang, J. 234 and 246 nm AlN-Delta-GaN Quantum Well Deep Ultraviolet Light-Emitting Diodes. *Appl. Phys. Lett.* **2018**, *112* (1), 011101.

(22) Islam, S. M.; Protasenko, V.; Lee, K.; Rouvimov, S.; Verma, J.; Xing, H.; Jena, D. Deep-UV Emission at 219 nm from Ultrathin MBE GaN/AlN Quantum Heterostructures. *Appl. Phys. Lett.* **2017**, *111* (9), 091104.

(23) Kobayashi, H.; Ichikawa, S.; Funato, M.; Kawakami, Y. Self-Limiting Growth of Ultrathin GaN/AlN Quantum Wells for Highly Efficient Deep Ultraviolet Emitters. *Adv. Opt. Mater.* **2019**, *7* (21), 1900860.

(24) Bayerl, D.; Islam, S.; Jones, C. M.; Protasenko, V.; Jena, D.; Kioupakis, E. Deep Ultraviolet Emission from Ultra-Thin GaN/AlN Heterostructures. *Appl. Phys. Lett.* **2016**, *109* (24), 241102.

(25) Sarwar, A. T. M. G.; May, B. J.; Chisholm, M. F.; Duscher, G. J.; Myers, R. C. Ultrathin GaN Quantum Disk Nanowire LEDs with Sub-250 nm Electroluminescence. *Nanoscale* **2016**, *8* (15), 8024−8032.

(26) Funato, M.; Kaneta, A.; Kawakami, Y.; Enya, Y.; Nishizuka, K.; Ueno, M.; Nakamura, T. Weak Carrier/Exciton Localization in InGaN Quantum Wells for Green Laser Diodes Fabricated on Semi-Polar {2021} GaN Substrates. *Appl. Phys. Express* **2010**, *3* (2), 021002.

(27) Mickevičius, J.; Jurkevičius, J.; Kazlauskas, K.; Žukauskas, A.; Tamulaitis, G.; Shur, M. S.; Shatalov, M.; Yang, J.; Gaska, R. Stimulated Emission Due to Localized and Delocalized Carriers in $Al_{0.35}Ga_{0.65}N/Al_{0.49}Ga_{0.51}N$ Quantum Wells. *Appl. Phys. Lett.* **2012**, *101* (4), 041912.

(28) Shan, M.; Zhang, Y.; Tran, T. B.; Jiang, J.; Long, H.; Zheng, Z.; Wang, A.; Guo, W.; Ye, J.; Chen, C.; Dai, J.; Li, X. Deep UV Laser at 249 nm Based on GaN Quantum Wells. *ACS Photonics* **2019**, *6* (10), 2387−2391.

(29) Ngo, T. H.; Gil, B.; Valvin, P.; Damilano, B.; Lekhal, K.; De Mierry, P. Internal Quantum Efficiency in Yellow-Amber Light Emitting AlGaN-InGaN-GaN Heterostructures. *Appl. Phys. Lett.* **2015**, *107* (12), 122103.

(30) Chichibu, Sf; Onuma, T.; Sota, T.; DenBaars, S. P.; Nakamura, S.; Kitamura, T.; Ishida, Y.; Okumura, H. Influence of InN Mole Fraction on the Recombination Processes of Localized Excitons in Strained Cubic $In_xGa_{1-x}N$/GaN Multiple Quantum Wells. *J. Appl. Phys.* **2003**, *93* (4), 2051−2054.

(31) Sun, Y. J.; Brandt, O.; Cronenberg, S.; Dhar, S.; Grahn, H. T.; Ploog, K. H.; Waltereit, P.; Speck, J. S. Nonpolar $In_xGa_{1-x}N$/GaN (1−100) Multiple Quantum Wells Grown on $\gamma$−$LiAlO_2$ (100) by Plasma-Assisted Molecular-Beam Epitaxy. *Phys. Rev. B: Condens. Matter Mater. Phys.* **2003**, *67* (4), 041306.

(32) Onuma, T.; Chakraborty, A.; Haskell, B. A.; Keller, S.; DenBaars, S. P.; Speck, J. S.; Nakamura, S.; Mishra, U. K.; Sota, T.; Chichibu, S. F. Localized Exciton Dynamics in Nonpolar (11−20) $In_xGa_{1-x}N$ Multiple Quantum Wells Grown on GaN Templates Prepared by Lateral Epitaxial Overgrowth. *Appl. Phys. Lett.* **2005**, *86* (15), 151918.

(33) He, H.; Yu, Q.; Li, H.; Li, J.; Si, J.; Jin, Y.; Wang, N.; Wang, J.; He, J.; Wang, X.; Zhang, Y.; Ye, Z. Exciton Localization in Solution-Processed Organolead Trihalide Perovskites. *Nat. Commun.* **2016**, *7* (1), 10896.

(34) Ko, T. S.; Lu, T. C.; Wang, T. C.; Lo, M. H.; Chen, J. R.; Gao, R. C.; Kuo, H. C.; Wang, S. C.; Shen, J. L. Optical Characteristics of A-Plane InGaN/GaN Multiple Quantum Wells with Different Well Widths. *Appl. Phys. Lett.* **2007**, *90* (18), 181122.

(35) Narukawa, Y.; Kawakami, Y.; Fujita, S.; Fujita, S.; Nakamura, S. Recombination Dynamics of Localized Excitons in $In_{0.2}Ga_{0.8}N$-$In_{0.05}Ga_{0.95}N$ Multiple Quantum Wells. *Phys. Rev. B: Condens. Matter Mater. Phys.* **1997**, *55* (4), R1938−R1941.

(36) Mohanta, A.; Thareja, R. K. Photoluminescence Study of ZnCdO Alloy. *J. Appl. Phys.* **2008**, *103* (2), 024901.

(37) Xu, S. J.; Liu, W.; Li, M. F. Direct Determination of Free Exciton Binding Energy from Phonon-Assisted Luminescence Spectra in GaN Epilayers. *Appl. Phys. Lett.* **2002**, *81* (16), 2959−2961.

(38) Gourdon, C.; Lavallard, P. Exciton Transfer between Localized States in $CdS_{1-x}Se_x$ Alloys. *Phys. Status Solidi B* **1989**, *153* (2), 641−652.

(39) Feng, S.-W.; Cheng, Y.-C.; Chung, Y.-Y.; Yang, C. C.; Lin, Y.-S.; Hsu, C.; Ma, K.-J.; Chyi, J.-I. Impact of Localized States on the Recombination Dynamics in InGaN/GaN Quantum Well Structures. *J. Appl. Phys.* **2002**, *92* (8), 4441−4448.

(40) Pavesi, L. Influence of Dispersive Exciton Motion on the Recombination Dynamics in Porous Silicon. *J. Appl. Phys.* **1996**, *80* (1), 216−225.



https://doi.org/10.1021/acsphotonics.1c00090
*ACS Photonics* 2021, 8, 1264−1270